

# A NEW METABOLISM MODEL FOR HUMAN SKELETAL MUSCLE

Dayu Lv and Bill Goodwine

Department of Aerospace and Mechanical Engineering, University of Notre Dame, Notre Dame, IN 46556 USA  
dlv@nd.edu, jgoodwin@nd.edu

Keywords: Glucose; Insulin; Skeletal Muscle; Metabolism.

Abstract: The human body metabolic regulatory system is very complex, containing thousands of metabolites involved in biochemical reactions. Glucose metabolism is one of the key procedures maintaining daily energy balance. Mobility of glucose is implemented by glucose transporters with different transporting characteristics locally, which are distributed in cells of brain, liver, pancreas, kidney and skeletal muscle, *etc.* This paper presents a component of a new model that is focused on skeletal muscle which consume energy consistently due to either slight movement or high-energy demanded activities, such as running or swimming. This paper presents a mathematical model where glucose, insulin, glucose-6-phosphate (G6P), *etc.* are introduced and described by ordinary differential equations.

## 1 INTRODUCTION

This paper presents a new model for the metabolic regulation of glucose in skeletal muscle in humans. It is part of a larger effort to develop a detailed whole-body human metabolic regulation model. Modeling of such systems is useful for several reasons. First, the mathematical structure of an accurate model will provide concise insight into the relevant physiology and also the pathophysiology of disease. Second, it will allow for inexpensive “experimentation” or biosimulation, which if predictive, can serve as a supplement to, and perhaps provide guidance to, *in vivo* and *in vitro* experimentation.

Of course this work is motivated by the epidemic of diabetes, which is a disease characterized by a failure to regulate blood glucose level. Many models have been constructed to describe glucose mobility in humans. What distinguishes this work from others is the scope, or dimension, of the model.

For many years, people have been investigating pathways of carbohydrates metabolism in order to establish mathematical models to reflect biology and control mechanisms. Composed of glucose, insulin and fatty acids (Srinivasan et al., 1970), a model was proposed to explain a two-hour metabolism respond-

ing to IV infusions of glucose, insulin, *etc.* Later, another hormone, glucagon, was added to a glucose-insulin system, (Cobelli et al., 1982). A few years ago, the mass of  $\beta$ -cells was connected to the system of glucose and insulin (Topp et al., 2000). Others were interested at kinetic properties of hormones, particularly insulin. A three-compartment insulin model was introduced (Sherwin et al., 1974). It was composed of a plasma compartment, a quick compartment equilibrating with plasma and a slower one. Also the pulsative characteristic of insulin was well simulated (Tolić et al., 2000).

Although many models have been proposed, they are mainly restricted to metabolites without reflecting transporters’ activities. In contrast, the model presented in this paper includes details regarding effects of, for example, various glucose transporters (GLUTs) in different organs, as well as *G6P*, which plays a key role in metabolism participating glycogenesis, glycogenolysis and glycolysis.

## 2 MODEL CONSTRUCTION

Skeletal muscle is actively involved in daily life. So the initial focus of our investigation into modeling

whole-body glucose metabolism will be skeletal muscle. This model is constituted of two main parts: the interstitial fluid space (*IFS*) and the intracellular space (*ICS*). In the *IFS*, cells are surrounded by a liquid environment for nutrition exchange. *Via* diffusion, glucose passes through capillaries to the *IFS*, then enter the *ICS* carried by GLUT4. In the *ICS*, glucose is converted to G6P for storage and utilization. Glycogen can also break down to form G6P.

## 2.1 Intercellular Transport

The mechanism for glucose transport in the *IFS* illustrated in Figure 1. It is assumed to diffuse through capillaries into the *IFS* and the direction is determined by the difference of glucose concentration between them,

$$f_{gs} = K_{01} \times ([G] - [G]_{si}), \quad (1)$$

where  $f_{gs}$  is positive for glucose out of plasma.

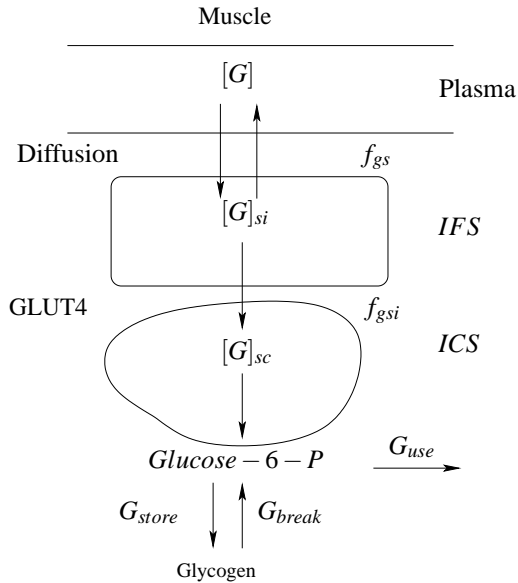


Figure 1: Three compartments of skeletal muscle.

Mediated by GLUT4, glucose is carried into the *ICS* following the Michaelis-Menton kinetics with  $V_{\max} = 1.0$  mmol/kg-muscle/min and  $K_m = 5.7$  mM in basal state (Perriott et al., 2001). Insulin and exercise may stimulate more GLUT4 activity. The rates of insulin stimulation can be determined from (Sarbacia et al., 1992), and exercise from (Fujimoto et al.,

2003) and are given by

$$In_V = \frac{1.4331}{1 + e^{-0.2473 \times \lg([In]/(16.7 \times 10^{-10})) - 3.271}} \quad (2)$$

$$Ex_{xV} = \frac{4.4531}{1 + e^{-198.5 \times (\dot{V}_{O_2}/\dot{V}_{O_2 \max}) + 60.95}} + 1, \quad (3)$$

$$V_{\max} = 1.0 \times Mass \times In_V \times Ex_{xV}, \quad (4)$$

where  $[In]$  represents insulin concentration in plasma,  $In_V$  represents the insulin effect on  $V_{\max}$  and  $Ex_{xV}$  represents the exercise effect on  $V_{\max}$ . Consequently, the glucose exchange amount between the *IFS* and the *ICS* is

$$f_{gsi} = -V_{\max} \frac{[G]_{si}}{K_m + [G]_{si}}, \quad (5)$$

where  $[G]_{sc}$  and  $[G]_{si}$  represents the glucose concentration in the *ICS* and the *IFS* respectively,  $f_{gsi}$  represents the rate which is positive for glucose transported out of the *ICS*.

In the model, insulin concentration is only considered in plasma, which is stimulated by increasing glucose concentration determined by dose-response on the secretion of insulin from isolated human islets of Langerhans (Frayn, 2003) and the data are fitted as

$$In_g = \left( \frac{79.21}{1 + e^{-1.934 \times [G] + 10.52}} + 29.84 \right) \times \frac{n \times 0.7}{V_p \times 60}, \quad (6)$$

where  $In_g$  represents the glucose stimulation on insulin secretion (mU/l/min),  $n$  represents the number of Langerhans, approximately one million (Frayn, 2003) assuming 70% of which are  $\beta$ -cells and  $V_p$  represents the plasma volume.

To describe the degradation of insulin ( $In_d$ , mU/l/min), the idea of half-life is implemented as

$$In_d = [In] \times e^{-K_{02} \times t}, \quad (7)$$

where  $[In]$  represents insulin concentration in plasma and  $K_{02}$  represents the half-life coefficient (assuming  $K_{02} = 20$ ). Then the dynamics of insulin concentration is

$$\frac{d[In]}{dt} = In_d + In_g. \quad (8)$$

## 2.2 Intracellular Space

After glucose uptake, it enters the intracellular metabolic process illustrated in Figure 2. The construction is based on the energy balance where the concentration of ATP remains almost constant (Frayn,

2003). G6P is generated from glucose and glycogen, and utilized through aerobic and anaerobic processes.

### 2.2.1 ATP Conservation

To meet the energy need of *Work* (mol/min), ATP is generated from aerobic and anaerobic glycolysis, the difference between which is the amount of ATP produced. Assuming oxygen is fully utilized by muscle, generating about 30 mol ATP from 1 mol G6P and 6 mol oxygen (*Aerobic* - mol/min, G6P consumed) while in anaerobic glycolysis (*Anaerobic*, mol/min, G6P consumed), only 2 mol ATP produced from 1 mol G6P. And converting glucose to G6P (*Rate*<sub>1</sub>, mol/min, G6P produced) and synthesis of G6P to glycogen (*Syn* - mol/min, glycogen produced) are consuming energy. The energy of *Work* can be expressed as metabolic rate (Frayn, 2003). It is important to be noted about the Randle-cycle, competition between glucose and fatty acids. Under different intensities of exercises, the proportion of fuels utilization between glucose and FFA is changing. For example, under rest or light housework, the proportion of glucose as a fuel is providing about 10% of required energy while during swimming it will increase to about 70%.

$$ATP_{O_2} = \frac{1.429 \times 5}{32} \times \dot{V}_{O_2}, \quad (9)$$

$$Aerobic = \frac{1.429}{32 \times 6} \times \dot{V}_{O_2}, \quad (10)$$

where the oxygen has the density of 1.429 g/l and mole mass of 32 g/mol. Then *Anaerobic*, the needed rate of G6P for anaerobic glycolysis can be calculated from

$$ATP_{O_2} - Rate_1 + Anaerobic \times 3 - Syn \times 20 = Work, \quad (11)$$

where *Rate*<sub>1</sub> represents the rate from glucose to G6P and *Syn* represents the synthesis rate of glycogen.

### 2.2.2 Glycogen Conservation

It is determined by the synthesis and breakdown rates,

$$Syn - Dwn = \Delta(GLY). \quad (12)$$

### 2.2.3 G6P Conservation

Glycogen is a highly branched polymer that can be looked on as a set of multi-G6Ps. In this model, the proportion of glycogen to G6P is assumed to be 1:10 and the change of G6P is given by

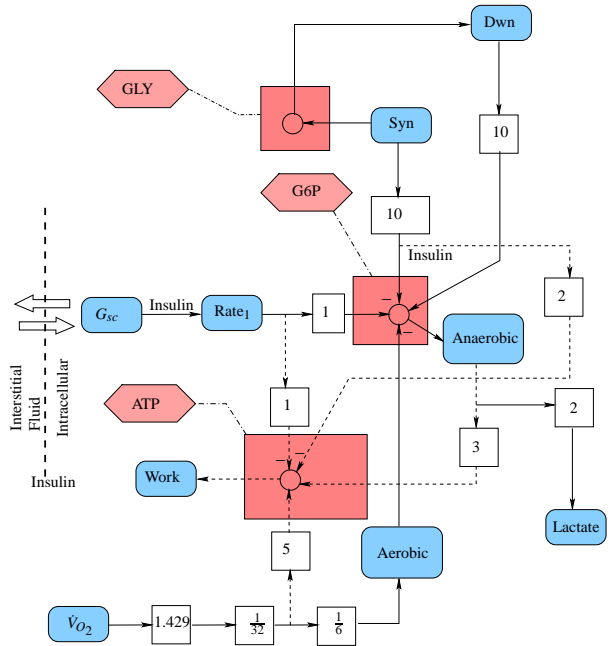


Figure 2: ATP Metabolism in Muscle

$$\Delta G6P = Rate_1 + 10Dwn - 10Syn - Aerobic - Anaerobic. \quad (13)$$

### 2.2.4 Variables

- *Rate*<sub>1</sub> is the hexokinase(*HK*) rate on converting glucose to G6P. Under 456 pM of insulin, *Rate*<sub>1</sub> was determined as 0.0048 mmol/kg-muscle/min (Rothman et al., 1992). Here are some assumptions:

1. *Rate*<sub>1</sub> is a sigmoidal function of insulin concentration;
2. *Rate*<sub>1</sub> is a sigmoidal function of [G6P];
3. *Rate*<sub>1</sub> is a sigmoidal function of [G]<sub>sc</sub>.

So the equations for *Rate*<sub>1</sub> are:

$$R_0 = 1.5 \times Mass, \quad (14)$$

$$In_R = \frac{2}{1 + e^{(-[I] + 40.0)/20}}, \quad (15)$$

$$G6P_R = \frac{2}{1 + e^{([G6P] - 0.12 \times Mass / V_{sc})/10}}, \quad (16)$$

$$G_{sc_R} = \frac{2}{1 + e^{-[G]_{sc} + 3.0}}, \quad (17)$$

$$Rate_1 = R_0 \times In_R \times G6P_R \times G_{sc_R}, \quad (18)$$

where *R*<sub>0</sub> is the basal value, *Mass* represents muscle weight, *In*<sub>R</sub>, *G6P*<sub>R</sub> and *G*<sub>sc</sub><sub>R</sub> represents their

effects on  $Rate_1$  respectively,  $[In]$ ,  $[G6P]$  and  $[G]_{sc}$  represents concentrations respectively,  $V_{sc}$  represents the volume of the  $ICS$ .

- The synthesis rate of glycogen,  $Syn$ , is determined by the concentration of glycogen from assumption and G6P, insulin fitted from the data (Kelley and Mandarino, 1990), in Table 1.

$$GLY_{syn} = \frac{1}{1 + e^{[GLY] - 0.95 \times [GLY]_{max}}}, \quad (19)$$

$$In_{syn} = \frac{2}{1 + e^{-2.2765 \times \lg \frac{[In]}{[In]_0}}} \times \frac{2}{1 + e^{0.3517 \times \lg \frac{[G6P]}{[G6P]_0}}}, \quad (20)$$

$$G6P_{syn} = 0.15 \times e^{\lg \frac{[G6P]}{[G6P]_0}}, \quad (21)$$

where  $[GLY]$  and  $[GLY]_{max}$  represents current and maximum glycogen concentration,  $In_{syn}$  and  $G6P_{syn}$  represents their effects on  $Syn$  respectively. So refer to the data,  $[In] = 28.2 \pm 4.2$  pM,  $[G6P] = 0.133 \pm 0.014$  mM, glycogen synthesis rate (mM/hr) was

$$Syn_1 = \begin{cases} 15.8 \pm 1.7, & [GLY] < 35 \text{ mM} \\ 2.9 \pm 0.2, & [GLY] > 35 \text{ mM} \end{cases} \quad (22)$$

(Price et al., 1996). In the model, we set  $Syn_0 = Syn_1 \times 8$  for reasonable simulation results.

$$Syn = Syn_0 \times In_{syn} \times G6P_{syn} \times GLY_{syn}. \quad (23)$$

Table 1: Insulin(Basal: 9.6 mU/l; Clamp  $77 \pm 3$ mU/l) and G6P (0.1mM; 10mM) effects on  $Syn$ .

Activity	Basal	Clamp
0.1 mM	$1.59 \pm 0.29$	$2.82 \pm 0.43$
10 mM	$6.14 \pm 0.62$	$7.21 \pm 0.67$

- The breakdown rate of glycogen,  $Dwn$ , is determined by G6P, glycogen and insulin concentrations. Design their effects on  $Dwn$  from hypothesis,  $In_{dwn}$ ,  $G6P_{dwn}$  and  $GLY_{dwn}$  as follows

$$In_{dwn} = \frac{2}{1 + e^{[In] - 20.0}}, \quad (24)$$

$$G6P_{dwn} = \frac{2}{1 + e^{[G6P] - 1.8}}, \quad (25)$$

$$GLY_{dwn} = \frac{1}{1 + e^{-[GLY] + 0.1 \times [GLY]_{max}}}, \quad (26)$$

where  $[In]$ ,  $[G6P]$ ,  $[GLY]$  and  $[GLY]_{max}$  represents

the concentrations of insulin, G6P, glycogen and maximum glycogen. Assume variables of needed G6P ( $G6P_1$ ) and of test ( $test_1$ ):

$$G6P_1 = Anaerobic + Aerobic + 10Syn \quad (27)$$

$$test_1 = G6P_1 - 0.5 \times \text{current G6P}. \quad (28)$$

If  $test_1$  is near or less than zero, which means current  $G6P$  is enough for consumption, set the rate (mol/min) as Equation 29 and else as Equation 30,

$$Dwn_0 = 0.02, \quad (29)$$

$$Dwn_0 = test_1 \times 30 \times 10^{-3} / dt. \quad (30)$$

Then the function of glycogen breakdown rate is

$$Dwn = Dwn_0 \times In_{dwn} \times G6P_{dwn} \times GLY_{dwn}. \quad (31)$$

### 3 SIMULATION RESULTS

Assuming glucose clamp  $[G] = 5$  mM, the simulations are finished via Matlab<sup>®</sup> with the following activity plans shown in Figure 3, 4 and 5.

- 4 hours rest;
- 1hr rest + 40min light housework + 2hr20min rest;
- 1hr rest + 40min swimming + 2hr20min rest.

For the plan of swimming, we also simulate it in higher glucose level  $[G] = 7$  mM and  $[G] = 14$  mM, the dynamics are demonstrated in Figure 6 and 7. Note that in Figure 7, intracellular glucose concentration increase rapidly at the last part of simulation, which is due to the saturation of muscle glycogen and  $G6P$ , and it may bring about critical health problems.

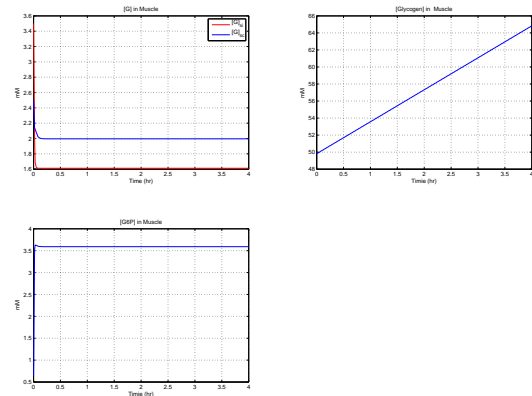


Figure 3: 4hr rest.

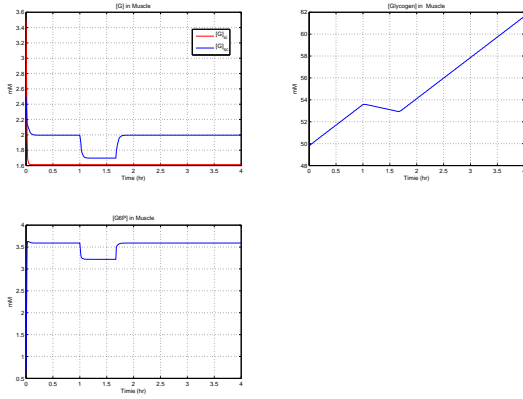


Figure 4: 1hr rest + 40min light housework + 2hr20min rest.

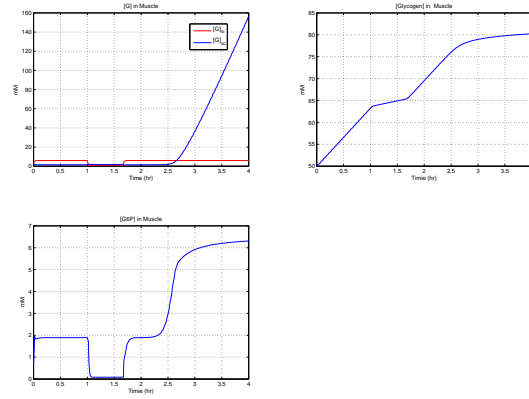


Figure 7:  $[G] = 14$  mM, swimming.

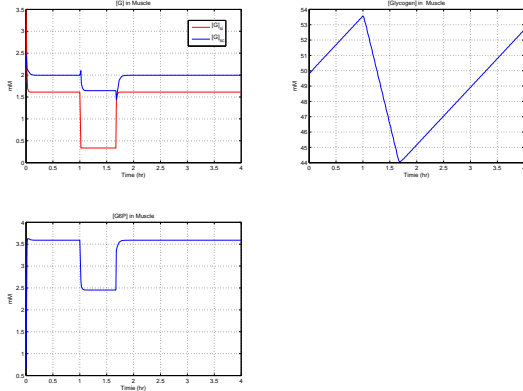


Figure 5: 1hr rest + 40min swimming + 2hr20min rest.

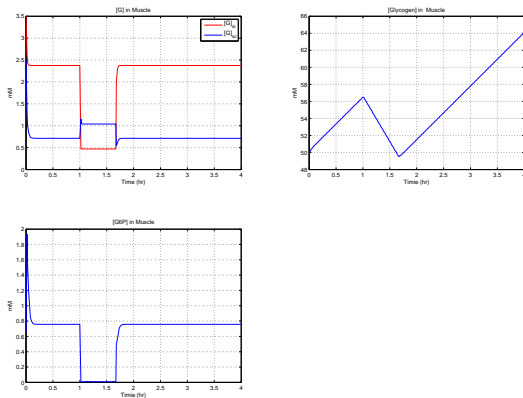


Figure 6:  $[G] = 7$  mM, swimming.

## 4 CONCLUSION AND PERSPECTIVES

In this paper, we have presented a mathematical metabolism model in human muscle. It is based on the kinetics of glucose transporters, GLUT4 and also considers the key role of *G6P*, whose regulation will determine the flow between storage and utilization. It works well in simulations. Under different activities, it reflects the interrelationships among glucose, insulin, *G6P* and glycogen.

The model has some limitations which we are currently addressing. First, the role of the glucose transporter GLUT1, with different kinetics is not yet considered. This transporter clearly plays a role in the basal state. Second, insulin concentration is considered only in plasma for simplification. And third, experiment data are still needed for a few of the equations. We indicated throughout the paper where a numerical value had to be assumed. Subsequent work will include a series of numerical experiments to better define the value, or range of values, that are feasible for such parameters.

In future work, the dynamics of insulin will be investigated and improved. Its resistance due to lasting high glucose level may be considered. Also, during exercises, increased level of lactate may be connected to other organs, such as liver. The overall goal, as mentioned previously, is a whole-body model expressed at a level of detail and fidelity similar to that for the muscle presented in this paper.

## ACKNOWLEDGEMENTS

Partial support from the Center for Applied Mathematics of University of Notre Dame and the Notre Dame Faculty Research Program are gratefully acknowledged.

## References

- Cobelli, C. et al. (1982). An integrated mathematical model of the dynamics of blood glucose and its hormonal control. *Mathematical Biosciences*, 58:27–60.
- Frayn, K. N. (2003). *Metabolic Regulation: A Human Perspective*. Blackwell Science Ltd, Oxford, 2nd edition.
- Fujimoto, T. et al. (2003). Skeletal muscle glucose uptake response to exercise in trained and untrained men. *Med. Sci. Sports Exerc.*, 35:777–783.
- Kelley, D. E. and Mandarino, L. J. (1990). Hyperglycemia normalizes insulin-stimulated skeletal muscle glucose oxidation and storage in noninsulin-dependent diabetes mellitus. *J. Clin. Invest.*, 86:1999–2007.
- Perriott, L. M. et al. (2001). Glucose uptake and metabolism by cultured human skeletal muscle cells: rate-limiting steps. *Am. J. Physiol. Endocrinol Metab.*, 281:72–80.
- Price, T. B. et al. (1996). Nmr studies of muscle glycogen synthesis in insulin-resistant offsprings of parents with non-insulin-dependent diabetes mellitus immediately after glycogen-depleting exercise. *Proc. Natl. Acad. Sci. USA*, 93:5329–5334.
- Rothman, D. L. et al. (1992). <sup>31</sup>P nuclear magnetic resonance measurements of muscle glucose-6-phosphate. *J. Clin. Invest.*, 89:1069–1075.
- Sarabia, V. et al. (1992). Glucose transport in human skeletal muscle cells in culture. *J. Clin. Invest.*, 90:1386–1395.
- Sherwin, R. S. et al. (1974). A model of the kinetics of insulin in man. *J. Clin. Invest.*, 53:1481–1492.
- Srinivasan, R. et al. (1970). A mathematical model for the control mechanism of free fatty acid-glucose metabolism in normal humans. *Computers and Biomedical Research*, 3:146–166.
- Tolić, I. M. et al. (2000). Modeling the insulin-glucose feedback system: the significance of pulsatile insulin secretion. *J. Theor. Biol.*, 207:361–375.
- Topp, B. et al. (2000). A model of  $\beta$ -cell mass, insulin, and glucose kinetics: pathways to diabetes. *J. Theor. Biol.*, 206:605–619.

$G/[G]$	mmol/mM	Glucose amount/concentration in plasma.
$G_{si}/[G]_{si}$	mmol/mM	Glucose amount/concentration in interstitial space.
$G_{sc}/[G]_{sc}$	mmol/mM	Glucose amount/concentration in intracellular space.
$G6P/[G6P]$	mmol/mM	G6P amount/concentration
$[In]$	mU/l	Insulin concentration.
$\dot{V}_{O_2}/\dot{V}_{O_2\max}$	l/min	Oxygen consumption rate/Maximum.
$Mass$	kg	Skeletal muscle weight,
$n$	N/A	Number of Langerhans
$V_{si}/V_{sc}$	1	Volume of interstitial space /intracellular space.
$V_b/V_p$	1	Blood/Plasma Volume.
$GLY/GLY_{\max}$	mM	Glycogen concentration /Maximum concentration.
$V_{\max}$	mmol/min	Maximum reaction rate.
$K_m$	mM	Michaelis constant.
$K_{01}$	l/min	Diffusion coefficient.
$K_{02}$	N/A	Insulin half-life coefficient.
<i>Aerobic</i>	mol/min	aerobic glycolysis rate.
<i>Anaerobic</i>	mol/min	anaerobic glycolysis rate.
<i>Syn</i>	mol/min	Glycogen synthesis rate.
<i>Dwn</i>	mol/min	Glycogen breakdown rate.

$[G]$	5
$[G]_{si}$	3.5
$[G]_{sc}$	2.5
$G6P$	$0.12 \times Mass$
<i>Body weight</i>	70
$Mass$	45% of <i>Body weight</i>
$n$	$10^6$
$[In]$	10
$\dot{V}_{O_2}$	Percentage of $\dot{V}_{O_2\max}$ : rest - 10% light housework - 25% swimming - 75%
$V_{si}$	10% of $Mass$
$V_{sc}$	$0.1852 \times Mass$
$V_b$	5
$V_p$	55% of $V_b$
$GLY_{\max}$	1% of $Mass$
$K_m$	5.7
$K_{01}$	2
$K_{02}$	20

## APPENDIX

The variables, parameters and initial values are shown in this appendix.